Volume 1 | Number 1 | Jan 2013 | Pages 1–100

Nanoscale

www.rsc.org/nanoscale

ROYAL SOCIETY OF CHEMISTRY

ROYAL SOCIETY OF CHEMISTRY

www.rsc.org/nanoscale

Nanoscale

ARTICLE

Effect of nanovaccine chemistry on humoral immune response kinetics and maturation

Shannon L. Haughney[a‡], Kathleen A. Ross[a‡], Paola M. Boggiatto[b], Michael J. Wannemuehler[b], and Balaji Narasimhan[a*]

Acute respiratory infections represent a significant portion of global morbidity and mortality annually. There is a critical need for efficacious vaccines against respiratory pathogens. To vaccinate against respiratory disease, pulmonary delivery is an attractive route because it mimics the route of natural infection and can confer both mucosal and systemic immunity. We have previously demonstrated that a single dose, intranasal vaccine based on polyanhydride nanoparticles elicited a protective immune response against *Yersinia pestis* for at least 40 weeks after immunization with F1-V. Herein, we investigate the effect of nanoparticle chemistry and its attributes on the kinetics and maturation of the antigen-specific serum antibody response. We demonstrate that manipulation of polyanhydride nanoparticle chemistry facilitated differential kinetics of development of antibody titers, avidity, and epitope specificity. The results provide new insights into the underlying role(s) of nanoparticle chemistry in providing long-lived humoral immunity and aid in the rational design of nanovaccine formulations to induce long-lasting and mature antibody responses.

Introduction

Acute respiratory infections represent a significant portion of global morbidity and mortality annually.[1,2] With the alarming increase in multi-drug resistant pathogens and the threat of aerosolized bioterrorism agents, there is an urgent need for the development of safe and efficacious vaccines against respiratory pathogens.[3,4] To vaccinate against respiratory disease, intranasal and pulmonary delivery are attractive routes because intranasal or inhaled vaccines can confer both mucosal and systemic immunity, and deliver antigen to immune inductive sites within the lung that can result in increased protection.[5,6] Recombinant protein technology has led to the development of protective antigens against many respiratory pathogens, often based on surface proteins of viruses and bacteria.[7,8] It is often noted, however, that antigen delivered alone does not induce protective immunity, and therefore, requires the use of adjuvants.[9,10]

Polyanhydride nanoparticle-based vaccines (i.e., nanovaccines) have previously been demonstrated to be a safe[11] and efficacious delivery platform for protein antigens.[12,13] These biodegradable polymers demonstrate pathogen-mimicking properties that adjuvant poorly immunogenic subunit proteins and enhance the immune response.[12] Additionally, particle chemistry may be tailored to stabilize labile proteins as well as to control the rate of protein release.[14] A single intranasal dose of a polyanhydride nanovaccine formulation based on F1-V, a recombinant fusion protein of *Yersinia pestis* that has been shown to be a protective antigen against pneumonic plague[15], was demonstrated to provide protective immunity in mice up to 40 weeks after vaccination.[12]

Previously, we have described the deposition, distribution, and prolonged presence of antigen delivered in the context of polyanhydride nanoparticles at early time points (i.e., 2 to 48 hours) after intranasal administration.[16] These nanoparticles were based on 1,6-bis(*p*-carboxyphenoxy) hexane (CPH) and 1,8-bis(*p*-carboxyphenoxy)-3,6-dioxaoctane (CPTEG). While the initial interactions between antigen and antigen presenting cells (APCs) are important in laying a foundation for vaccine efficacy, the chemistry of the nanovaccine formulation plays an important role in the continual recruitment of APCs and for the development of high antibody titers with high avidity. In this work, we systematically analyzed the effect of nanoparticle chemistry on antigen availability, sustained internalization of antigen by immune cells, and the kinetics and maturation of the humoral immune response.

Materials and Methods

Materials

The materials used for monomer synthesis include sodium hydroxide, hydrobenzoic acid, dibromohexane, 1-methyl-2-pyrrolidinone, triethylene glycol, and sebacic acid (SA) (Sigma Aldrich, St. Louis, MO). Acetone, sulfuric acid, potassium carbonate, dimethyl formamide, toluene, acetonitrile, N,N-dimethylacetamide, and acetic acid were purchased from Fisher Scientific (Fairlawn, NJ). 4-*p*-fluorobenzonitrile used in the synthesis of CPTEG monomer was purchased from Apollo Scientific (Cheshire, UK). Acetic anhydride, ethyl ether, petroleum ether, chloroform, methylene chloride, and hexane used in acetylation and polymerization were purchased from Fisher Scientific. Deuterated chloroform and dimethyl sulfoxide were used in ^{1}H NMR analysis of the polymers and monomers (Cambridge Isotope Laboratories, Andover, MA). Pentane and methylene chloride used in nanoparticle synthesis were purchased from Fisher Scientific.

F1-V fusion protein (BEI Resources, Manassas, VA) was conjugated to the fluorescent label Vivo Tag 680 (Perkin Elmer, Waltham, MA). Flow cytometry utilized anti-mouse antibodies and their respective isotypes for PerCP-Cy5.5-conjugated anit-CD11c, biotinylated anti-CD324, streptavidin eFluor 710 (eBioscience, San Diego, CA), PE-CF594-conjugated anti-CD11b (BD Bioscience, San Jose, CA), and PE-Cy7-conjugated anti-F4/80 (BioLegend, San Diego, CA).

Polymer synthesis

The CPH and CPTEG monomers were synthesized as described previously[17–20]. Pre-polymers of CPH and SA were synthesized from monomers as described previously[18,19]. Copolymers based on CPH, CPTEG, and SA were synthesized using melt condensation as described by Kipper et al. and Torres et al[17,18]. Polymer purity and molecular weight were determined using ^{1}H NMR (Varian VXR300).

Nanoparticle synthesis

The Vivo Tag 680 fluorescent label was conjugated to F1-V fusion protein according to manufacturer instructions (Perkin Elmer). Briefly, 10 µL of Vivo Tag 680 was added per mg of F1-V and incubated at room temperature for 1 h. Excess unconjugated Vivo Tag 680 was removed using a 5 kDa MWCO dialysis microcentrifuge tube. The protein was lyophilized overnight at -40˚C under vacuum. The F1-V loaded polyanhydride nanoparticles were formulated using an anti-solvent precipitation method as described previously[13]. Polymer and 2% (w/w) F1-V were dissolved in methylene chloride at a concentration of 20 mg/mL. The solution was sonicated (Vibra-Cell^{TM}, Sonics & Materials, Newton, CT) at an output of 40 Hz to ensure a homogenized mixture. The resulting solution was rapidly poured into pentane at a solvent:non-solvent ratio of 1:250 at room temperature for CPH:SA formulations or at -40°C for CPTEG:CPH copolymers due to the lower glass transition temperature of the CPTEG-containing copolymers[17]. Nanoparticles were collected via vacuum filtration and characterized using scanning electron microscopy (FEI Quanta SEM, Hillsboro, OR). Particle size distribution was determined from resultant images using ImageJ (Version 1.46r, NIH, Bethesda, MD) software and found to be consistent with previous work[20,21].

Mice

Five to six week old C57BL/6 mice were obtained from Harlan Laboratories (Haslett, MI). Mice were housed under specific pathogen-free conditions where all bedding, caging, water, and feed were sterilized prior to use. All studies were conducted with the approval of the Iowa State University Institutional Animal Care and Use Committee.

Immunization protocol

Mice (between 7 and 9 weeks of age) were anesthetized with a 100 µL injection of a solution containing 20 mg/mL ketamine and 1 mg/mL xylazine and immunized intranasally. Experimental groups consisted of 10 µg of F1-V encapsulated into 500 µg of 50:50 CPTEG:CPH, 20:80 CPTEG:CPH, or 20:80 CPH:SA nanoparticles with 40 µg of soluble F1-V delivered concurrently in 50 µL of PBS, 50 µg of F1-V delivered with 10 µg MPLA derived from *Salmonella enterica* serotype Minnesota Re 595 (Sigma Aldrich), or 50 µg of F1-V alone. While the animals were anesthetized, saline suspensions of the polyanhydride nanovaccines, protein alone, or protein with MPLA were delivered to the mice using a 100 µL pipettor fitted with a pipet tip to deliver a total of 50 µL of fluid to the animal. Approximately 25 µL was delivered through each nare of the nose. Sterile PBS was administered to all control animals. Mice were euthanized at 14, 36, or 63 days post-immunization. Samples were collected from four mice per group per time point and the experiment was repeated resulting in a total of eight mice per group per time point. The soluble protein alone and PBS control groups contained a total of four animals per treatment group.

Ex vivo lung imaging

Mice were euthanized to measure the amount of protein remaining in the lung at 14, 36, and 63 days after intranasal immunization. A lung perfusion with 5 mL of sterile PBS was performed to reduce background autofluorescence caused by red blood cells and the lungs were then excised. An *in vivo* live animal imaging system (Carestream Multispectral FX, Rochester, NY) was used to measure the fluorescence of antigen remaining in the lungs. A white light image (2 s exposure) followed by a fluorescent image (60 s exposure) with an excitation of 670 nm and a 750 nm emission filter was used.

Images were analyzed with ImageJ software. Mean fluorescence intensity (MFI) was calculated using the fluorescent lung images. A region of interest was drawn around the fluorescent image and the mean was recorded. Background was then subtracted from each sample and a MFI value was obtained. For the *ex vivo* lung images (Figure 1), background was subtracted from the fluorescent images with a rolling ball radius of 40, the images were smoothed, and the false-color look-up table "fire" was applied. White light images were adjusted to have the same minimum and maximum values and a z-projection of the two images was created.

Multi-spectral imaging flow cytometry

After imaging, lung samples were incubated in Hank's balanced salt solution (HBSS) with 1 mg/mL of collagenase D and 60 U/mL of DNase II for 20 min at 37°C. Tissue was then homogenized to a single cell suspension using a gentleMACS™ dissociator (Miltenyi Biotec, Cambridge, MA). The cellular suspensions were centrifuged at 250 rcf for 30 s to remove large debris. The supernatants were then passed through a 40 μm filter and the filtrate was then centrifuged at 250 rcf for 10 min at 4°C to pellet the cells. Remaining red blood cells in the lung homogenates were lysed with ACK lysis buffer (150 mM ammonium chloride, 10 mM potassium bicarbonate, 0.1 mM EDTA), and cells were centrifuged once more before enumeration using a Coulter counter (Beckman Coulter, Indianapolis, IN). Cells were washed once in buffer (2% heat inactivated fetal bovine serum and 0.1% sodium azide in PBS) and re-suspended in 60 μL of 1% paraformaldehyde (PFA) in PBS. Samples were analyzed using an ImageStreamX (Amnis, Seattle, WA) with a 658 nm laser and 600-745 nm emission filter to measure the internalized F1-V using IDEAS® software (Amnis).

Flow cytometry

Single cell suspensions were prepared as described above. Cell solutions were incubated with 0.1 mg/mL rat IgG and 10 μg/mL mouse anti-CD16/32 to prevent non-specific binding of fluorescent antibodies. Cells were surface-labeled with specific monoclonal antibodies against CD11c, CD11b, CD324, and F4/80 for 30 min. After washing, the labeled cell samples were re-suspended in 100 μL stabilizing fixative (BD Biosciences) and analyzed using a FACS Canto flow cytometer (BD Biosciences, San Jose, CA). Analysis of the flow cytometric data was performed with FlowJo software (Treestar, Inc., Ashland, OR).

Anti-F1-V serum antibody titers and avidity assays

Antibody titers were determined using an enzyme-linked immunosorbent assay (ELISA) as described elsewhere [13]. Briefly, high-binding microtiter plates were coated with 100 μL of F1-V (0.5 μg/mL) in PBS and incubated overnight at 4°C. F1-V coated microtiter plates were incubated with blocking buffer (0.05 M PBS with 0.05% Tween 20 (PBS-T) supplemented with 2.5% powdered skim milk) for 2 h at room temperature before washing three times with PBS-T. Serum from immunized mice was added to the first well at a 1:200 dilution in PBS containing 1% goat serum and three-fold serial dilutions were performed. After incubating at 4°C overnight, plates were washed three times with PBS-T. Alkaline phosphatase-conjugated goat anti-mouse IgG (heavy and light chain) (Jackson ImmunoResearch, West Grove, PA) was added at a concentration of 1 μg/mL and incubated for 2 h at room temperature. Plates were washed again and 1 mg/mL of alkaline phosphatase substrate (Fisher Scientific, Pittsburgh, PA) dissolved in 50 mM sodium carbonate, 2 mM magnesium chloride buffer (pH 9.3) was added for colorimetric development. The optical density (OD) was recorded after 30 min at 405 nm. All the samples were tested in technical replicates of two. Herein, we define titer as the serum dilution value that produced an OD greater than twice the background (i.e., saline) value. Avidity assays were performed as described above for ELISA. After overnight incubation with 100 μL per well serum at a 1:200 dilution, a 5 M solution of sodium thiocyanate in a 0.1 M sodium phosphate buffer was added to the first well and serially diluted two-fold five times (i.e., for a final dilution of 1:32). Six control wells were used per sample and received sodium phosphate buffer alone. The solution was incubated for 15 min before washing thoroughly. The remainder of the assay followed the steps described above for ELISA. A relative avidity index was calculated by using an exponential fit of sodium thiocyanate serial dilutions to determine the concentration at which the OD is 50% of that of the non-treated wells containing the 1:200 diluted serum sample.

Overlapping peptide array assay

In order to measure the immune response to specific F1-V epitopes, an overlapping peptide array (BEI Resources) assay was performed. High-binding microtiter plates were coated with individual F1-V peptides at a concentration of 5 μg/mL in PBS. The ELISA protocol described above was followed with a single serum dilution of 1:200 used for each sample. The optical density (OD) was recorded at 405 nm after incubating for 2 h at room temperature.

Statistics

Statistical significance in Figures 1 and 3 was determined by one-way analysis of variance (ANOVA) followed by Tukey's post-test using GraphPad Prism software (Version 6.01, GraphPad Software, Inc., La Jolla, CA). A logarithmic transformation was performed on the antibody titer data presented in Figure 2 before determining statistical significance by ANOVA with a Bonferroni correction. In cases where the antibody titer was undetectable, a value of one-half the limit of detection was used. P-values less than or equal to 0.05 were considered significant.

Table 1. Size and polydispersity of polyanhydride nanoparticles

Chemistry	Size (nm)	PDI
20:80 CPTEG:CPH	120 +/- 55	0.17
50:50 CPTEG:CPH	151 +/- 63	0.15
20:80 CPH:SA	324 +/- 162	0.17

Results and Discussion

Immunization with polyanhydride nanovaccines induced prolonged availability of antigen in the lung for up to 63 days after administration

In order to compare the antigen availability and the kinetics of the humoral immune response induced by the different nanoparticle chemistries, a 50 µg dose of F1-V was used in all the vaccine formulations. A comparison of the nanoparticle sizes and polydispersity is shown in Table 1. The use of nanoscale particles is motivated by previous work from our laboratories on the deposition and clearance kinetics of micron-sized vs. nm-sized particles in the lung[22]. These studies suggest optimum pulmonary deposition and cellular uptake of particles in the 300-500 nm size range, without inducing any adverse tissue responses. Vaccination of mice using a combination of 40 µg soluble F1-V along with 50:50 CPTEG:CPH nanoparticle-encapsulated F1-V (10 µg) in a single intranasal dose has previously been demonstrated to induce protection against lethal challenge with *Y. pestis*[12,13]. The rationale of using a soluble bolus (40 µg) of antigen along with a portion (10 µg) encapsulated within the nanoparticles is that the soluble bolus rapidly primes the B cell response, while the encapsulated portion is released slowly over several weeks to sustain that immune response. In the present studies, F1-V was fluorescently labeled with Vivo Tag 680 in order to track the persistence of the protein in the lung after intranasal administration. Anesthetized C57B/6 mice were administered a single, intranasal dose of a given vaccine formulation and separate groups of mice were euthanized at 14, 36, and 63 days in order to quantify the remaining fluorescence in the excised lungs followed by flow cytometric assessment of F1-V associated with or internalized by dissociated lung cells.

Figure 1 demonstrates the persistence of F1-V within the lung following its administration in soluble form or encapsulated into polyanhydride nanoparticles. The data also demonstrate the differential effect of nanoparticle chemistry on antigen availability. Consistent with our previous work[16], F1-V adjuvanted with MPLA was essentially cleared from the lung by day 14. In contrast, F1-V administered in the context of the polyanhydride nanovaccine formulations continued to persist in the lung as a function of nanoparticle chemistry. The decay of fluorescence associated with nanoparticle clearance kinetics from the lung is qualitatively consistent with previous work examining antigen release kinetics from polyanhydride nanoparticles *in vitro*[23]. The nanoparticles based on the CPH-

rich chemistries (i.e., 20:80 CPTEG:CPH and 50:50 CPTEG:CPH) maintained visible and measurable fluorescence for at least 63 days after immunization indicating the prolonged availability of antigen within the lung. In contrast, nanoparticles based on the SA-rich 20:80 CPH:SA showed a marked decrease in fluorescence within the lung 36 days after immunization and returned to baseline levels by 63 days.

Quantification of antigen internalization within the lung was used to investigate the combined effects of nanoparticle chemistry and antigen availability. Nanoparticles based on SA-rich chemistries were demonstrated previously to be more readily internalized by APCs in comparison to particles based on CPH-rich chemistries[20,24,25]. However, SA-rich chemistries have faster erosion and release kinetics than CPH-rich chemistries[24], and, therefore, result in reduced antigen availability at later time points. Consistent with these observations, mice immunized with the 20:80 CPH:SA nanovaccine formulation demonstrated a qualitatively higher, though not statistically significant, percentage of lung cells that internalized antigen on day 14 post-immunization (Figure S1). However, by 36 and 63 days post-immunization, the percentage of cells containing internalized F1-V delivered in the 20:80 CPH:SA nanovaccine formulation had further decreased. In contrast, lung cells from mice administered the hydrophobic and CPH-rich 20:80 CPTEG:CPH nanovaccine continued to demonstrate the presence of internalized antigen for at least 63 days, albeit at low levels. This observation can be attributed to the slower erosion profile of CPH-rich chemistries[26], which enables sustained antigen release and availability.

Polyanhydride nanovaccines elicit sustained high titer antibody responses

The data in Figure 1 provides evidence regarding the kinetics of F1-V availability within the lung after intranasal immunization with polyanhydride nanovaccines. These data also suggest that F1-V is continuously present within lung cells for at least 36 days regardless of the formulation administered. Next, new insights are presented on the combined effects of polymer chemistry and antigen availability on the serum antibody response to F1-V. The data in Figure 2 demonstrates that the kinetics of the resultant anti-F1-V IgG antibody titer was affected by the choice of polymer chemistry, while antigen availability had less of an impact on the antibody titer over time. The antibody titer elicited by all the formulations studied was statistically significant in comparison to that induced by the soluble F1-V alone at each time point. Other than the IgG responses induced by 50:50 CPTEG:CPH, the serum antibody response for mice immunized with all other formulations demonstrated serum antibody titer $\geq$ 50,000 by day 36; however, the day 63 titer in these groups indicated that the F1-V-specific IgG response began to wane. However, the mice that received the 50:50 CPTEG:CPH nanovaccine showed progressively increasing serum antibody titer through the nine weeks of this study. While detectable in the lung for 63 days

(Figure 1), the animals that received soluble F1-V alone did not develop a measurable antibody titer demonstrating that the presence of immunogen alone is not sufficient and that an appropriate adjuvant is necessary to induce the development of a F1-V-specific antibody response.

Antigen availability and release kinetics affects antibody avidity

The availability of antigen may not only facilitate sustained antibody titer, but drive the development of avid antibodies as well. Similar to antibody titer, the evolution of the avidity of F1-V-specific IgG was found to be a function of the nanovaccine polymer chemistry (Figure 3). Nanovaccines based on 20:80 CPTEG:CPH and 20:80 CPH:SA nanoparticles induced antibody avidities similar to MPLA. Although these formulations developed highly avid antibodies by 36 days post-immunization, there were no further increases in avidity at later time points. In contrast, the serum of mice that received the amphiphilic 50:50 CPTEG:CPH nanovaccine showed a significant increase in avid F1-V-specific IgG antibody at each time point. Only the mice administered the 50:50 CPTEG:CPH nanovaccine formulation showed continued maturation of the IgG avidity, as evidenced by the fact that the avidity was statistically different at each subsequent time point. These differences in avidity may be attributed in part to the differences in the antigen release kinetics from these polymers[14,17,26] and, therefore, antigen availability. It is likely that the 20:80 CPH:SA nanoparticles release antigen too rapidly to stimulate the continual affinity maturation (i.e., sequentially higher avidity) of the F1-V-specific antibody response. Despite a similar antibody response induced by 20:80 CPH:SA nanovaccine, the most hydrophobic 20:80 CPTEG:CPH nanoparticles may release antigen too slowly such that there may not be sufficient F1-V to elicit an ever maturing antibody response. In contrast, the 50:50 CPTEG:CPH nanoparticles must exhibit a release rate of antigen that results in a sequential improvement of the avidity of the F1-V-specific IgG response.

Polyanhydride nanovaccines result in broader epitope specificity

The ability of vaccines to induce responses towards a broad spectrum of epitopes may enhance protection. Because the antibody avidity (Figure 3) is the summation of the antibody response towards all epitopes, an overlapping peptide array of the F1-V antigen was used to determine the antibody response to specific epitopes induced by each immunization regimen as shown by the heat map in Figure 4. Consistent with the antibody titer and avidity responses depicted in Figures 2 and 3, the responses to specific epitopes were highly dependent upon the nanoparticle chemistry and the kinetics of antigen release. The number of peptides recognized by serum IgG (i.e., peptides which showed an optical density (OD) value above background, or OD value ≥ 0.5) at each time point is shown across the bottom of the heat map. Serum antibodies from mice

receiving the 20:80 CPTEG:CPH nanovaccine showed increased recognition in terms of the number of epitopes recognized by serum antibody between days 14 and 36 post-immunization; however, this response saturated by 36 days post-immunization. Likewise, the number of recognized epitopes, while initially broad, waned over time in the case of serum from the mice that received the 20:80 CPH:SA nanovaccine. Interestingly, the 50:50 CPTEG:CPH nanovaccine induced an IgG response that continued to expand the epitopes recognized over time, which corroborates the increases in antibody titer and avidity discussed previously.

The ability to induce antibodies specific for a broad spectrum of epitopes is no doubt important for long-term protection; however, the V1 and V2 epitopes in particular have been shown to be important for protection against *Y. pestis* in C57BL/6 mice[27,28]. The data in Figure 5 compares the immune response to these two dominant epitopes in response to each of the formulations, with an OD value with a greater than 1.5-fold change from saline controls defined as epitope recognition[29]. The immune response to these dominant epitopes induced by the 50:50 CPTEG:CPH nanovaccine exhibited a time dependent evolution and the optical density increased over time as the immune response narrowed to these epitopes. This type of kinetics was not observed with any of the other nanovaccine formulations nor with MPLA. Similar responses were observed for the F18 epitope (data not shown), noting that the addition of responses to the F1 antigen enhanced the protection provided by the V antigen[15].

In this work, different polyanhydride nanovaccine formulations were systematically examined for their ability to affect *in vivo* antigen availability and the resultant induction of a humoral immune response. While all the formulations examined produced similar antigen-specific antibody titers, the kinetics of the F1-V-specific immune response varied when antigen was delivered in the context of the different polymer nanovaccine chemistries. Building upon our previous work[12,13,16], the studies presented herein shed new light upon the complex relationship(s) between polyanhydride nanoparticle chemistry and the kinetics and maturation of the induced humoral immune response.

Of the three nanoparticle formulations evaluated, the 20:80 CPH:SA chemistry is the least hydrophobic. As a result, the 20:80 CPH:SA nanoparticles have the fastest polymer degradation kinetics, leading to the release of a vast majority of the protein within one month[26,30,31]. In agreement with the above *in vitro* observations of release kinetics, the fluorescently-labeled F1-V was nearly undetectable in the lung by 36 days post-immunization indicating that the 20:80 CPH:SA nanoparticles had eroded and released its payload (Figure 1). In addition to faster antigen release, the clearance of F1-V encapsulated within the 20:80 CPH:SA nanoparticles can also be attributed to the enhanced internalization of these particles (Figure S1). As it is the antigen that is labeled in this

work (rather than the particle), it is important to state that relative to the disappearance of the soluble protein alone, it is clear that the persistent F1-V in this group is due its encapsulation into 20:80 CPH:SA nanoparticles, which is in turn was cleared most rapidly among the polyanhydride chemistries tested. These observations support previous work in which nanoparticles composed of SA-rich chemistries were rapidly internalized in comparison to CPH-rich chemistries[20,24,25].

While the 20:80 CPH:SA nanovaccine formulation more rapidly induced the development of antibody titers compared to the other nanoparticle formulations,(Figure 2), both the titer as well as the avidity of the antibody reached their peak values at 36 days post-immunization (Figures 2 and 3, respectively). The number of F1-V epitopes recognized by the antibody from mice administered the 20:80 CPH:SA nanovaccine decreased with time (Figure 4). This observation can be linked to the kinetics of the antibody titer and avidity of the response to the 20:80 CPH:SA nanovaccine formulation, which remain unchanged between the two later time points. The rapid release and clearance of antigen, and therefore decrease in antigen availability, may affect the ability of the 20:80 CPH:SA nanovaccine formulation to sustain long-term protective immune responses. In addition, the decreased hydrophobicity and rapid degradation of this polymer, leading to a similarly rapid waning of the pro-inflammatory cytokine response induced after implantation, may present fewer danger signals to the immune system in comparison with more hydrophobic chemistries[32]. We hypothesize that the reduced danger signal elicited by this formulation, coupled with its rapid clearance from the lung, may lead to the induction of short-lived plasma cells[33], which is consistent with the waning antibody titers and avidity as observed in Figures 2 and 3. Thus, it is likely the 20:80 CPH:SA nanovaccine formulation may be suitable for rapid induction of immunity, but not for induction of long-lived antigen-specific IgG, as suggested by the data.

In contrast, the CPH-rich nanovaccine formulations (i.e., 20:80 CPTEG:CPH and 50:50 CPTEG:CPH) are more hydrophobic and degrade more slowly, providing slower protein release kinetics[17] and prolonging the presence of antigen in the lung for at least 63 days as shown in Figure 1. However, the CPH-rich chemistries were also less readily internalized by lung cells than the SA-rich chemistries as shown in Figure S1 and in previous work[12,20]. The combination of the reduced internalization and slower degradation kinetics due to increased hydrophobicity enabled the CPH-rich nanovaccine formulations to provide sustained antigen presence. Together, these observations raise an important question on the effect of nanoparticle degradation and antigen availability on the generation and maintenance of humoral immune responses over time[32].

The antibody titer and avidity responses in mice administered the 20:80 CPTEG:CPH nanovaccine formulation reached their

maximum by 36 days post-immunization (Figures 2 and 3). The kinetics of these responses were similar to those observed in mice administered the 20:80 CPH:SA nanovaccine formulation, albeit with higher titers. We hypothesize that the hydrophobicity of the 20:80 CPTEG:CPH nanovaccine formulation may promote a more inflammatory environment, possibly leading to an increased response to the initial soluble bolus of antigen, which is consistent with previous observations[11]. We propose that the lower availability of antigen at later time points, after the depletion of the soluble portion of the vaccine, from this slowly degrading formulation is offset by the greater inflammatory milieu (i.e., enhanced adjuvanticity) provided by this more hydrophobic formulation. This combination of hydrophobicity-induced inflammation and slow yet continuous release of antigen may lead to the induction of longer lived plasma cells, which are important for long-term maintenance of the antibody titers[33-35]. In addition, mice receiving this formulation demonstrated a greater breadth in the epitope specificity of the humoral immune response in terms of the ability to recognize more antigen-specific epitopes over time (Figure 4), possibly due to the prolonged exposure to F1-V in the lung. Together, these data suggest that highly hydrophobic nano-carriers can be used to formulate vaccines that promote the maturation of potent and long-lived humoral immune responses.

The 50:50 CPTEG:CPH nanovaccine formulation has been demonstrated in our previous work to possess pathogen-mimicking abilities in terms of its internalization by APCs and its activation and induction of long-term protective immunity[12,24]. The antibody titers and the avidity of the antigen-specific IgG responses of mice that received the 50:50 CPTEG:CPH nanovaccine formulation continued to increase at each successive time point (Figures 2 and 3). In contrast to the other formulations, the mean levels of circulating antibody increased between 36 and 63 days after immunization only for the mice that received the 50:50 CPTEG:CPH nanovaccine formulation. We propose that this observation suggests that the immune response induced by the 50:50 CPTEG:CPH nanovaccine and the persistent presence of antigen would facilitate continual differentiation of B cells into long-lived plasma cells[33-35]. It is also important to note that memory B cells induced in early germinal centers typically develop broader antibody repertoires (i.e., greater avidity and increased epitope spread)[33-35] as suggested by the data in Figures 3 and 4. There are several other factors to consider when analyzing these observations. First, CPTEG-rich polymers have lower glass transition temperatures compared to the other polyanhydrides studied herein that likely contributes to particle agglomeration within the lung, leading to a reduced surface area to volume ratio and resulting in slower release of antigen and prolonged presence of F1-V[17,18]. Second, the alternating pattern (i.e., -CPTEG-CPH-CPTEG-CPH-CPTEG-) provided by the 50:50 CPTEG:CPH copolymer (because of its equal monomer reactivity ratios)[17] may be recognized by immune cells as a microbe-associated molecular pattern. As the

nanoparticles erode, an increased number of oligomeric chains are generated with molecular patterns that might mimic an increasing microbial burden as with a replicating pathogen or a replication-competent, live, attenuated vaccine. This is supported by previous work demonstrating protective immunity 40 weeks after a single intranasal immunization[12,13]. In light of these observations, we suggest that the pathogen-mimicking 50:50 CPTEG:CPH nanovaccine formulation more effectively primes the immune response and induces long-lived immunity.

Conclusions

The data presented in this work demonstrated that the intranasal administration of polyanhydride nanovaccine formulations with disparate erosion kinetics and degrees of hydrophobicity to mice induced antigen-specific antibody responses characterized by different kinetic profiles of titers and avidity as well as epitope specificities. While the prolonged availability of F1-V *in vivo* may play an important role in the development and maturation of protective antibody responses, the persistence of F1-V alone is *not* enough to drive an efficacious immune response. The differences observed in the humoral response in mice administered the various polyanhydride nanovaccine formulations can be attributed to the differences in polymer hydrophobicity, polymer degradation rates, the molecular patterns presented by the polymer backbone, the induction and complexity of inflammatory signals, and antigen availability. We hypothesize that all of these factors contribute to differential induction and maintenance of germinal centers that lead to long-lived serum antibody responses. An understanding of these aspects and their underlying role(s) in providing long-lived protective immunity in a single dose will be valuable to rationally design efficacious vaccines. These observations and hypotheses indicate that polyanhydride nanovaccines can be tailored based on polymer chemistry to control hydrophobicity, degradation kinetics, antigen availability, and inflammatory signals to induce the development of sustained and mature antibody responses, characterized by increasing antibody titers at late time points, the enhancement of antibody avidity, and a broadened epitope specificity with time.

Acknowledgements

Notes and references

[a] Department of Chemical and Biological Engineering, Iowa State University, Ames, IA 50011. E-mail: nbalaji@iastate.edu; tel.: +1 515 294 8019; fax: +1 515 294 2689.
[b] Department of Veterinary Microbiology and Preventive Medicine, Iowa State University, Ames, IA 50011.

1   J. P. Mizgerd, *Am J Respir Crit Care Med*, 2012, **186**, 824–9.
2   G. Nm, *Epidemiol Rev*, 1989, **12**, 149–78.
3   R. A. Greenfield, M. S. Bronze, *Drug Discov Today*, 2003, **8**, 881–8.
4   M. Galimand, A. Guiyoule, G. Gerbaud, B. Rasoamanana, E. Chanteau S, Carniel, et al, *N Engl J Med*, 1997, **337**, 677–81.
5   D. Lu, A. J. Hickey, *Expert Rev Vaccines*, 2007, **6**, 213–26.
6   H. O. Alpar, S. Somavarapu, K. N. Atuah, V. W. Bramwell, *Adv Drug Deliv Rev*, 2005, **57**, 411–30.
7   S. Sharma, T. K. S. Mukkur, H. A. E. Benson, Y. Chen, *J Pharm Sci*, 2009, **98**, 812-843.
8   Y. Yuki, H. Kiyono, *Expert Rev Vaccines*, 2009, **8**, 1083-1097.
9   M. Singh, D. O'Hagan, *Nat Biotechnol*, 1999, **17**, 1075–81.
10   J. H. Wilson-Welder, M. P. Torres, M. J. Kipper, S. K. Mallapragada, M. J. Wannemuehler, B. Narasimhan, *J Pharm Sci*, 2009, **98**, 1278–316.
11   L. Huntimer, A. E. Ramer-Tait, L. K. Petersen, K. A. Ross, K. A. Walz, C. Wang, et al, *Adv Healthc Mater*, 2013, **2**, 369–78.
12   B. D. Ulery, L. K. Petersen, Y. Phanse, C. S. Kong, S. R. Broderick, D. Kumar, et al, *Sci Reports*, 2011, **1**, 198, doi: 10.1038/srep00198.
13   B. D. Ulery, D. Kumar, A. E. Ramer-Tait, D. W. Metzger, M. J. Wannemuehler, B. Narasimhan, *PLoS ONE*, 2011, **6**, e17642, doi: 10.1371/journal.pone.0017642.
14   B. Carrillo-Conde, E. Schiltz, J. Yu, F. Chris Minion, G. J. Phillips, M. J. Wannemuehler, et al, *Acta Biomater*, 2010, **6**, 3110–9.
15   J. Hill, C. Copse, S. Leary, A. J. Stagg, E. D. Williamson, R. W. Titball, *Infect Immun*, 2003, **71**, 2234–8.
16   K. A. Ross, S. L. Haughney, L. K. Petersen, P. Boggiatto, M. J. Wannemuehler, B. Narasimhan, *Adv Healthc Mater*, 2014, **3**, 1071-77, doi: 10.1002/adhm.201300525.
17   M. P. Torres, B. M. Vogel, B. Narasimhan, S. K. Mallapragada, *J Biomed Mater Res A*, 2006, **76**, 102–10.
18   E. Shen, R. Pizsczek, B. Dziadul, B. Narasimhan, *Biomaterials*, 2001, **22**, 201–10.
19   M. J. Kipper, E. Shen, A. Determan, B. Narasimhan, *Biomaterials*, 2002, **23**, 4405–12.
20   B. D. Ulery, Y. Phanse, A. Sinha, M. J. Wannemuehler, B. Narasimhan, B. H. Bellaire, *Pharm Res*, 2009, **26**, 683–90.
21   B. Carrillo-Conde, E-H. Song, A. Chavez-Santoscoy, Y. Phanse, A. E. Ramer-Tait, N. L. B. Pohl, et al, *Mol Pharm*, 2011, **8**, 1877–86.
22   T. M. Brenza, L. K. Petersen, A. E. Ramer-Tait, M. J. Wannemuehler, B. Narasimhan. *Pharm Res* (2014, under review).
23   L. K. Petersen, Y. Phanse, A. E. Ramer-Tait, M. J. Wannemuehler, B. Narasimhan. *Mol Pharm,* 2012, **9**, 874-82.
24   L. K. Petersen, A. E. Ramer-Tait, S. R. Broderick, C-S. Kong, B. D. Ulery, K. Rajan, et al, *Biomaterials*, 2011, **32**, 6815–22.
25   B. R. Carrillo-Conde, A. E. Ramer-Tait, M. J. Wannemuehler, B. Narasimhan, *Acta Biomater*, 2012, **8**, 3618–28.
26   L. K. Petersen, C. K. Sackett, B. Narasimhan, *J Comb Chem*, 2010, **12**, 51–6.
27   J. Hill, S. E. Leary, K. F. Griffin, E. D. Williamson, R. W. Titball, *Infect Immun*, 1997, **65**, 4476–82.

28   J. K. Pullen, G. W. Anderson, S. L. Welkos, A. M. Friedlander, *Infect Immun*, 1998, **66**, 521–7.

29   Y. Phanse, B. R. Carrillo-Conde, A. E. Ramer-Tait, S. Broderick, C. S. Kong, K. Rajan, *Sci Reports*, 2014, **4**, 3775, doi: 10.1038/srep03775.

30   E. Shen, M. J. Kipper, B. Dziadul, M-K. Lim, B. Narasimhan, *J Controlled Release*, 2002, **82**, 115–25.

31   A. S. Determan, B. G. Trewyn, VS-Y. Lin, M. Nilsen-Hamilton, B. Narasimhan, *J Controlled Release*, 2004, **100**, 97–109.

32   S. Y. Seong, P. Matzinger, *Nat Rev Immunol*, 2004, **4**, 469-478.

33   M. Shapiro-Shelef, K. Calame, *Nat Rev Immunol*, 2005, **5**, 230–42.

34   M. J. Shlomchik, F. Weisel, *Immunol Rev*, 2012, **247**, 52-63.

35   K. L. Good-Jacobson, M. J. Shlomchik, *J Immunol*, 2010, **185**, 3117-3125.

List of Figures

Fig 1. Polyanhydride nanovaccines persisted in the lung for up to 63 days. Images represent fluorescence of remaining Vivo Tag 680 labeled F1-V antigen in excised lung tissue at the indicated time points. Mean fluorescence intensity (MFI) is represented graphically as the average of eight mice per group from a total of two independent experiments (days 14 and 36) and four mice per group from one experiment (day 63). Error bars represent the standard error of the mean. Letters represent statistical differences among formulations at one time point (e.g., comparing the MFI of the 50:50 CPTEG:CPH nanovaccine at day 36 to the 20:80 CPTEG:CPH nanovaccine at day 36). Asterisks represent statistical differences between time points within a single formulation ($p \leq 0.05$).

Fig 2. Polyanhydride nanovaccines induced high titer anti-F1-V antibody responses. Error bars represent the standard error of the mean ($n = 8$) from two independent experiments (days 14 and 36) and $n = 4$ from one experiment (day 63). The antibody titers elicited by all the formulations studied were statistically significant in comparison to that induced by the soluble formulation at each time point. Asterisks represent statistical differences between time points within a single formulation ($p \leq 0.0077$).

Fig 3. Polyanhydride nanovaccine formulations induced highly avid antibodies to F1-V. Error bars represent the standard error of the mean ($n = 8$) from two independent experiments (days 14 and 36) and $n = 4$ from one experiment (day 63). Asterisks represent statistical differences between time points within a single formulation ($p \leq 0.0084$).

Fig 4. Nanovaccine formulations resulted in enhanced epitope recognition by antibodies. The responses to eighty F1 and V peptides were evaluated by ELISA and are shown as a heat map, beginning at the top with the amino-terminal peptide and then moving down sequentially through the F1-V protein. The optical density of each peptide is indicated by a range of color from blue (no response) to red (maximum response). The number of reactive peptides (i.e., optical density (OD) value above background, or OD value ≥ 0.5) induced by each vaccine formulation at each time point is indicated below the heat map. Data presented is the average of eight individual mice for days 14 and 36, and four individual mice for the day 63 time point.

Fig 5. Evolution of the immune response to the immunodominant V1 and V2 peptides is affected by nanoparticle chemistry. The data is shown as a fold-change over saline. Data was collected from groups of animals for days 14 and 36 in two individual experiments and from four animals for day 63 in one experiment. Epitope recognition is defined as 1.5-fold or higher over saline. The dashed line represents a 1.5-fold change from saline controls for each peptide.
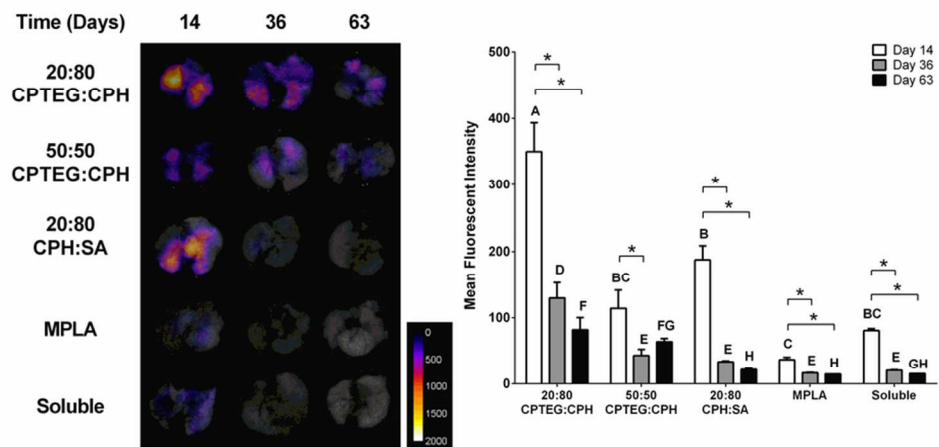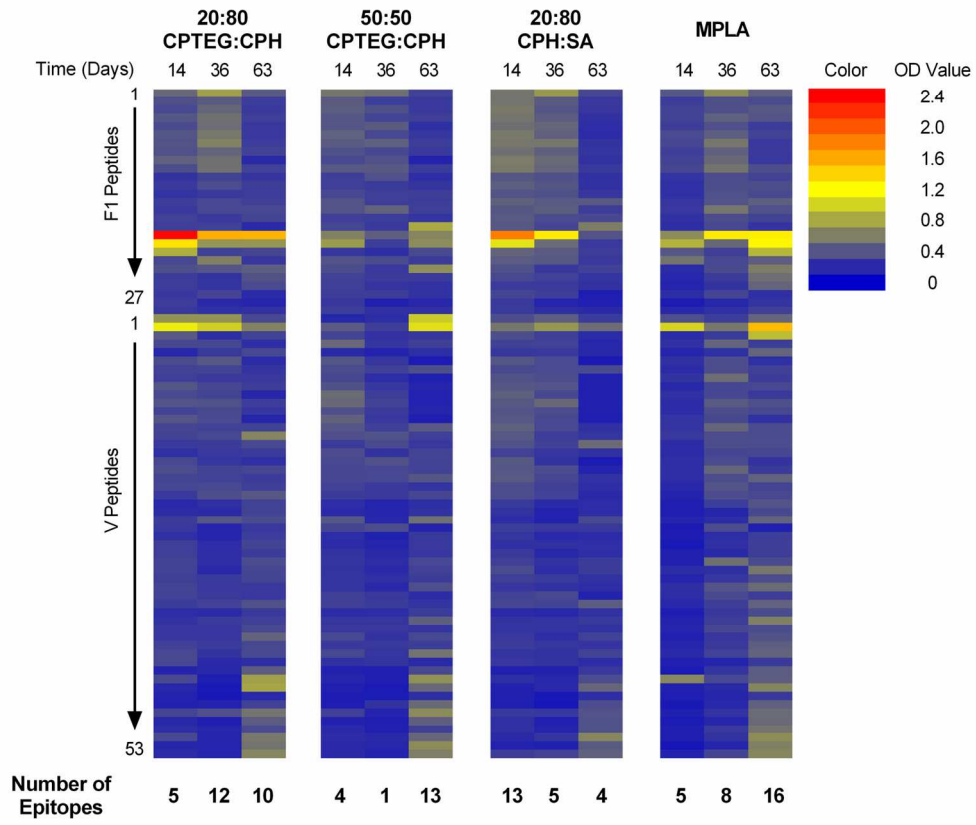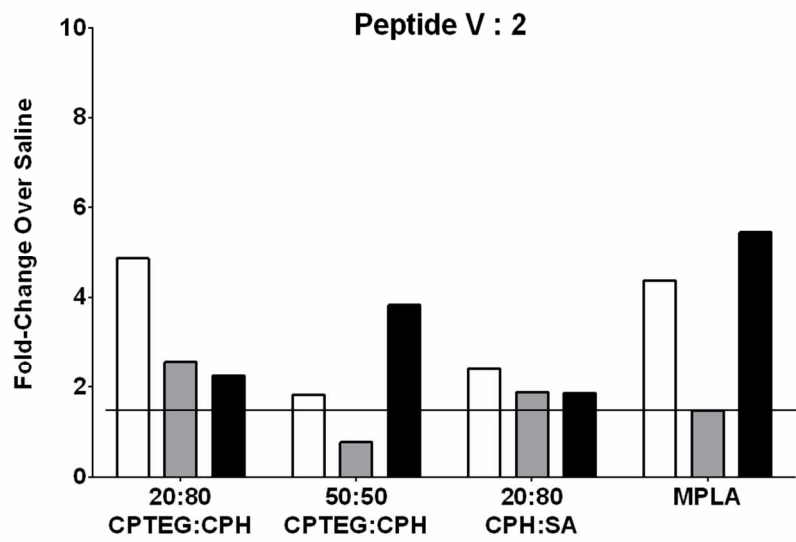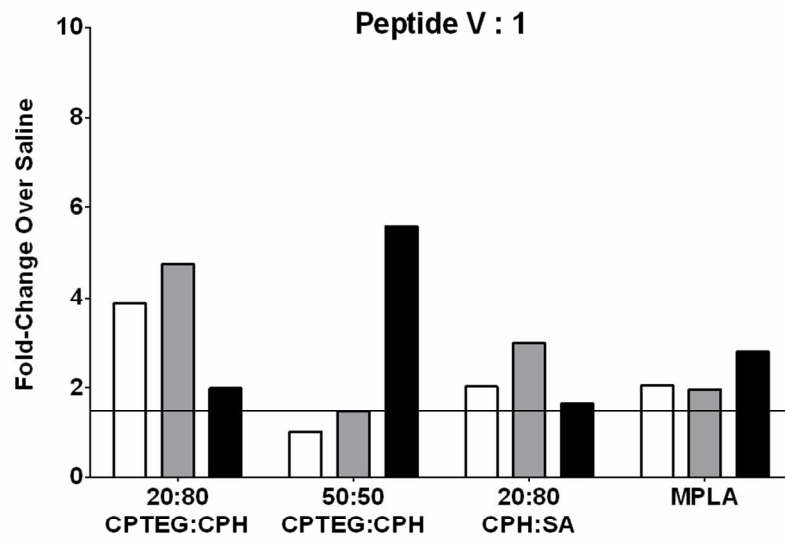
83x38mm (300 x 300 DPI)
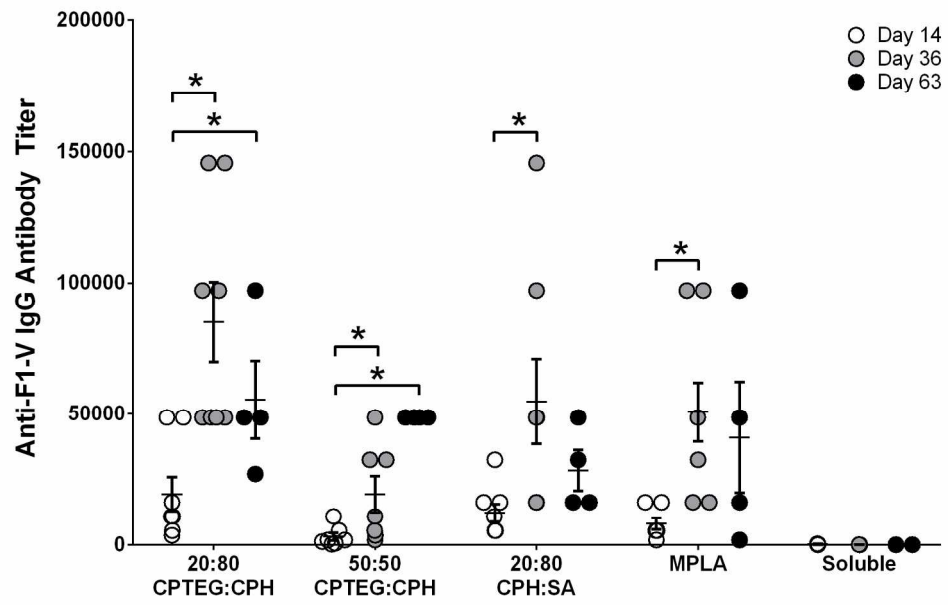
177x113mm (300 x 300 DPI)
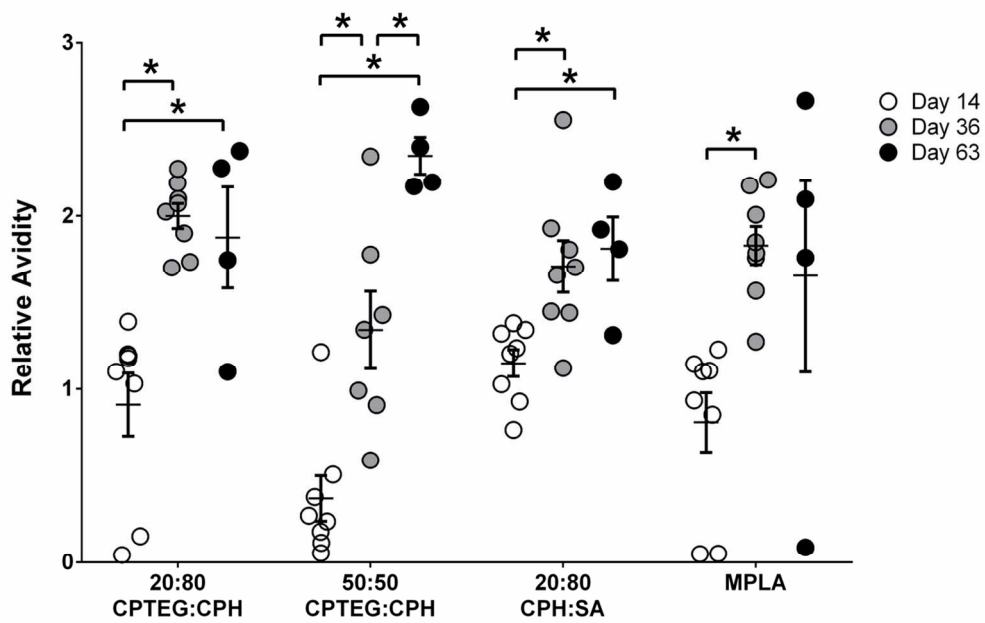
116x76mm (300 x 300 DPI)

150x127mm (300 x 300 DPI)

88x118mm (300 x 300 DPI)